

Development and characterization of p1025-loaded bioadhesive liquid-crystalline system for the prevention of *Streptococcus mutans* biofilms

Giovana Maria Fioramonti Calixto¹

Cristiane Duque²

Kelly Limi Aida²

Vanessa Rodrigues dos Santos²

Loiane Massunari²

Marlus Chorilli¹

¹School of Pharmaceutical Sciences, São Paulo State University (UNESP), Araraquara, São Paulo, Brazil; ²School of Dentistry, São Paulo State University (UNESP), Araçatuba, São Paulo, Brazil

Abstract: Formation of a dental biofilm by *Streptococcus mutans* can cause dental caries, and remains a costly health problem worldwide. Recently, there has been a growing interest in the use of peptidic drugs, such as peptide p1025, analogous to the fragments 1025–1044 of *S. mutans* cellular adhesin, responsible for the adhesion and formation of dental biofilm. However, peptides have physicochemical characteristics that may affect their biological action, limiting their clinical performance. Therefore, drug-delivery systems, such as a bioadhesive liquid-crystalline system (LCS), may be attractive strategies for peptide delivery. Potentiation of the action of LCS can be achieved with the use of bioadhesive polymers to prolong their residence on the teeth. In line with this, three formulations – polyoxypropylene-(5)-polyoxyethylene-(20)-cetyl alcohol, oleic acid, and Carbopol C974P in different combinations (F1C, F2C, and F3C) were developed to observe the influence of water in the LCS, with the aim of achieving in situ gelling in the oral environment. These formulations were assessed by polarized light microscopy, small-angle X-ray scattering, rheological analysis, and in vitro bioadhesion analysis. Then, p1025 and a control (chlorhexidine) were incorporated into the aqueous phase of the formulation (F + p1025 and F + chlorhexidine), to determine their antibiofilm effect and toxicity on epithelial cells. Polarized light microscopy and small-angle X-ray scattering showed that F1C and F2C were LCS, whereas F3C was a microemulsion. F1C and F2C showed pseudoplastic behavior and F3C Newtonian behavior. F1C showed the highest elastic and bioadhesive characteristics compared to other formulations. Antibiofilm effects were observed for F + p1025 when applied in the surface-bound salivary phase. The p1025-loaded nanostructured LCS presented limited cytotoxicity and effectively reduced *S. mutans* biofilm formation, and could be a promising p1025-delivery strategy to prevent the formation of *S. mutans* dental biofilm.

Keywords: liquid crystal, formulation, polymer, peptide, bacterium, dental caries

Correspondence: Giovana Maria Fioramonti Calixto; Marlus Chorilli
Department of Drugs and Medicines, School of Pharmaceutical Sciences, São Paulo State University – Campus Araraquara, Rodovia Araraquara-Jaú Km 1, Araraquara, São Paulo 14801-902, Brazil
Tel +55 16 3301 6961
Fax +55 16 3322 0073
Email calixtogmf@fcar.unesp.br/chorilli@fcar.unesp.br

Introduction

Streptococcus mutans is closely associated with the etiology of dental caries,^{1–3} which is still one of the most widespread diseases worldwide, affecting people of all ages throughout their lifetimes.⁴ It is considered a biofilm-dependent disease, because the pathogenic microbiota, which colonize and proliferate in dental biofilms, are the most important factor, along with a high-carbohydrate diet, for the onset and progression of the disease.^{5–8} Virulence factors, including the adhesin antigens I/II (Ag I/II), glucosyltransferases, and glucan-binding protein, improve the ability of *S. mutans* to adhere and accumulate in the dental biofilm.^{9–12}

Numerous studies have demonstrated the importance of immunoresponse against Ag I/II in human protection against *S. mutans* colonization.¹³ In vitro studies with Ag I/II-knockout *S. mutans* strains have shown decreased adhesion to hydroxyapatite on the enamel surface, suggesting that Ag I/II facilitates the adhesion of the bacteria.¹⁴ Downregulation of Ag I/II in biofilm cells is critical for initial biofilm formation, but not for established biofilms.¹⁵ These findings may provide useful information regarding the importance of Ag I/II as a tool for new strategies to control biofilm-mediated infections.¹⁶ In vitro assays of *S. mutans* adhesion to dental surfaces have identified that the salivary agglutinin present in human saliva is an Ag I/II receptor, mediating the binding between bacteria and teeth.¹⁷

Kelly et al identified amino acid residues 1025–1044 in the C-terminal region of Ag I/II as the adhesion epitope of this antigen.¹⁸ The synthetic peptide p1025 corresponding to these residues was able to inhibit in vitro binding between *S. mutans* adhesin and salivary agglutinin. p1025 also reduced the recolonizing of *S. mutans* in dental biofilm in vivo. Li et al demonstrated that a dentifrice containing p1025 decreased the adhesion of *S. mutans* hydroxyapatite surfaces covered by saliva.¹⁹

Several topical formulations are commonly employed for controlling dental biofilm formation, such as mouthwash, gels, dentifrices, and lozenges. However, these formulations are often characterized by limited drug retention in the oral cavity, and they tend to be rapidly dislodged, diluted, or removed, which can alter the efficacy of the active principles present in their composition, such as antimicrobial agents.²⁰ Therefore, numerous administrations are required to achieve and maintain effective levels of the drug.^{21–24} Therefore, the development of a drug-delivery nanosystem that provides controlled release of a drug retained for longer in the mucosa would be very advantageous.²⁴

Among all drug-delivery nanosystems, the liquid-crystalline system (LCS) has received considerable attention, because of its excellent potential to control the release of a wide range of biomolecules, including peptides.^{25–27} The LCS also stands out because it is formed by surfactants that form lamellar, hexagonal, and cubic crystalline liquid mesophases, by the gradual addition of solvents, such as water. The lamellar mesophase is a one-dimensional structure formed by parallel and planar layers of surfactant bilayers separated by layers of solvent. The hexagonal mesophase is formed by layers of surfactant and solvent that are arranged in the form of cylinders forming a two-dimensional structure. Finally, the cubic mesophase is formed by two networks of solvent channels surrounded by surfactant bilayers arranged in a three-dimensional organized structure.²⁸

Therefore, the gradual increase of water in the LCS increases the organization of the system structure, which results in an increase in viscosity of the formulation. As such, LCS are interesting for buccal drug administration, as liquid can be present, facilitating administration of the formulation, eg, by syringe. However, when it comes in contact with the oral environment, the LCS has the capacity to incorporate water from the saliva, becoming a more viscous LC mesophase; therefore, this in situ gelling characteristic allows for the administration of a liquid into the oral cavity via syringe that then becomes a viscous solution that adheres to the teeth for a long period.^{28,29}

An innovative strategy for further increasing residence time of the LCS on the tooth is to incorporate polyacrylic acid polymers in the aqueous phase, once these polymers produce viscous gels with high bioadhesion.³⁰ In this sense, we have investigated the bioadhesion of different polyacrylic acid polymers, such as Carbopol 971P, Carbopol 974P (C974), and polycarbophil, and results showed that the bioadhesion of C974 was highest.³¹ Jones et al investigated the bioadhesion of different gels for xerostomia treatment, and they also observed that the gel composed of C974 enhanced the residence time of the product.³² Thereby, the objectives of this study were to develop and characterize a nanostructured, bioadhesive LCS composed of C974 dispersion as the aqueous phase, oleic acid (OA) as the oily phase, and polyoxypropylene-(5)-polyoxyethylene-(20)-cetyl alcohol as the surfactant to incorporate the p1025 peptide and to evaluate its in vitro cytotoxicity and effect against the formation of *S. mutans* biofilm.

Materials and methods

Materials

PPG-5-Ceteth-20 (Procetyl AWS) was purchased from Croda (Campinas, Brazil). OA was purchased from Labsynth (Diadema, São Paulo, Brazil). The carbomer homopolymer type B (C974) was purchased from Lubrizol (Wickliffe, OH, USA). Peptide p1025 with sequence Ac-QLKTADL-PAGRDETTSFVLV-NH₂ (molecular weight 2,202.5 Da) was purchased from AminoTech Research and Development (Diadema, SP, Brazil). Chlorhexidine diacetate (Chx) was purchased from Sigma-Aldrich (St Louis, MO, USA). High-purity water was prepared with a Millipore Milli-Q Plus purification system, and its resistivity was 18.2 MΩ·cm.

Construction of ternary-phase diagram and preparation of formulations

A ternary-phase diagram was constructed at 25°C±0.5°C by weighing and mixing different amounts of polyoxypropylene-

(5)-polyoxyethylene-(20)-cetyl alcohol (PPG-5-Ceteth-20) as the surfactant, OA as the oil phase, polymeric dispersion containing 5% (w:w) C974P, and water as the aqueous phase. The final polymeric concentration in each formulation was 0.5% (w:w). The polymeric dispersion was prepared via dispersing 5% (w/w) C974P in water and homogenizing it at 2,000 rpm in a mechanical stirrer for approximately 10 minutes at 25°C±0.5°C. Following complete dissolution, the pH was adjusted to 6 with triethanolamine (Labsynth) and manual agitation. The pH of each final formulation was 5.5. Then, all formulations were visually classified as a transparent liquid system, translucent liquid system, transparent viscous system, translucent viscous system, opaque viscous system, or phase separation. The different regions in the phase diagram were then delineated. From these data, the formulations F1C, F2C, and F3C were selected for physicochemical characterization.²⁶

Structural features of the formulations

Polarized light microscopy

Polarized light microscopy (PLM) analyses were performed by placing a small amount of each formulation on a glass slide and covering it with a coverslip. Samples were analyzed using a Jenamed (Carl Zeiss Meditec AG, Jena, Germany), evaluating the homogeneity of the dispersion and observing the presence of anisotropy or isotropy at a magnification of 20× and temperature of 25°C.³³

Small-angle X-ray scattering

The structural arrangements of the LCSs were analyzed by small-angle X-ray scattering (SAXS) using Brazilian Synchrotron Light Laboratory (Campinas, Brazil) equipment with a type Si(111) monochromator at a wavelength of 1.608 Å that yields a horizontally focused beam. A vertical Pilatus 300K SAXS detector located at 858.45 mm from the sample and a multichannel analyzer 13 were employed to record the intensity of scattering vector q from 0.1 to 3.8 Å at 25°C. Scattering particles in the system without a sample were subtracted from the total intensity of the sample, as a function of the module of the scattering vector:

$$q = 4\pi \times \frac{\sin \theta}{\lambda} \quad (1)$$

where λ is the wavelength and θ the scattering angle. The intensities of all samples were measured in relative units, but a quantitative comparison of measurements was standardized under the same experimental conditions.²⁸

Rheological analysis

Rheological measurements were performed at 37°C±0.1°C in triplicate using a controlled-stress AR2000 rheometer (TA Instruments, New Castle, DE, USA) with parallel-plate geometry (40 mm diameter) and a sample gap of 200 μm. Formulation samples were carefully applied to the lower plate to minimize sample shearing and were allowed to equilibrate for 3 minutes prior to analysis.³⁰

Determination of flow properties

Flow properties were determined using a controlled shear-rate procedure ranging from 0.01 to 100 seconds and back. Each stage lasted for 120 seconds, with an interval of 10 seconds between the curves. Consistency and flow indices were determined from the power law described in Equation 2 for a quantitative analysis of flow behavior:

$$\tau = \kappa \times \gamma^n \quad (2)$$

where “ τ ” is shear stress, “ γ ” shear rate, “ κ ” consistency index, and “ n ” the flow index.

Oscillatory analyses

Oscillatory analyses were initiated by conducting a stress sweep to determine the viscoelastic region of the formulations. The stress sweep was carried out at a constant frequency of 1 Hz over a stress range of 0.1–10 Pa. A constant shear stress of 1 Pa was selected to perform the frequency sweep over a range of 0.1–10 Hz, which was within the previously determined linear viscoelastic region for all formulations. As such, the storage (G') and loss (G'') moduli were recorded. Variations in G' at low frequencies in a log–log plot of G'' versus ω followed the power law described in Equation 3, given by:

$$G' = S \times \omega^n \quad (3)$$

where G' is the storage modulus, S the formulation strength, ω the oscillation frequency, and n the viscoelastic exponent.

In vitro bioadhesion study

Preparation of disks

Six fresh bovine permanent central incisors were collected, scaled to remove periodontal tissue and other debris, and stored in 1% thymol solution at 4°C for 1 month until use. This research protocol was performed in accordance with the International Guidelines Principles for Biomedical Research involving animals (Council for International Organization of Medical Sciences-CIOMS/International Council for Laboratory Animal Science – ICLAS) and approved by the Ethical Committee

on the use of animals (FOA/UNESP, protocol 2014/00618). Teeth with enamel cracks, hypoplasia, and calculus in the middle third of the crown or other morphological alterations were excluded. Enamel blocks were cut transversally from the middle third of the buccal surface of each tooth using a water-cooled, double-faced diamond disk (KG Sorensen, Barueri, Brazil). Specimens were then rounded using a high-speed, water-cooled cylindrical diamond burr (1095; KG Sorensen) to obtain specimens with a diameter of 1 cm containing enamel. Teeth surfaces were polished with wet 200-grit silicon carbide paper (T469-SF Norton; Saint-Gobain Abrasives, Worcester, MA, USA) to normalize the surface.³⁴

Bioadhesion study

A TA-XT Plus texture analyzer (Stable Micro Systems, Godalming, UK) was used for tensile strength measurements. The tooth model was fastened to the upper movable probe with double-sided tape, and the formulation sample was located on the lower platform. Before the test, the tooth was immersed in artificial saliva. The upper probe was lowered until it made contact with the sample, and kept in contact without any additional force applied for 60 seconds. The probe was then raised at a speed of 0.5 mm/second, and the force needed for detachment was registered. The work of bioadhesive force (mN·s), which is proportional to the area under the force–time curve, was used to describe bioadhesive characteristics. Seven replicates were analyzed at 37°C±0.5°C.³⁰ The composition of the artificial saliva used was 8 g/L sodium chloride, 0.19 g/L of potassium monobasic phosphate (KH₂PO₄), and 2.28 g/L of disodium phosphate (Na₂HPO₄) with pH 6.8.³⁶

Microbiological evaluation

Preparation of the groups

p1025 was solubilized in sterile deionized water with 0.1% acetic acid (CH₃COOH) at a concentration of 1,000 µg/mL prior to use and stored in a freezer at –20°C until use. The positive-control group was Chx at 1 mg/mL. Peptide p1025 and Chx were incorporated into the aqueous phase of formulation F3C at a concentration of 1 mg/mL based on a previous study.⁵² The groups studied were p1025 and Chx solutions, F3C (F), F3C containing p1025 (F + p1025), and F3C containing Chx (F + Chx). F3C was diluted tenfold before incorporating Chx and p1025 to reduce the viscosity for biofilm assays.³⁶

Biofilm biomass assays

The effect of treatments on biofilm formation was studied following the methodology described in Ahn et al,³⁷ with some modifications in biofilm growth in the presence of

saliva proposed by Castillo.³⁸ Firstly, stimulated saliva was collected once from two healthy volunteers with good oral health in sterile tubes, after approval by the Human Research Ethics Committee of Araçatuba Dental School, Universidade Estadual Paulista, Brazil (CAAE 13079213.4.0000.5420). All volunteers whose saliva was used in this research provided informed consent. Volunteers were asked not to eat or drink for at least 2 hours prior to collection. The saliva from volunteers was mixed in equal proportions and centrifuged at 4,000× *g* for 10 minutes at 4°C to remove cell debris. After that, the supernatant was mixed with the buffered solution (0.05 M KCl, 0.02 M KPO₄, 0.02 M CaCl₂, and 0.02 M MgCl₂) at a ratio of 1:1 and 0.1 M phenylmethylsulfonyl fluoride (Sigma-Aldrich) was added. Clarified saliva was used after filter sterilization through a 0.22 µm-filter bottle (Corning, Corning, NY, USA). For the following experiments, each treatment (F + p1025, F + Chx, p1025, and Chx solutions [all at 1 mg/mL]) was diluted 1:3 in saliva.

Overnight cultures of *S. mutans* UA159 were transferred to prewarmed brain–heart infusion containing 1% glucose and grown at 37°C in 5% CO₂ to the mid-exponential phase (OD 0.5). The cultures were then diluted 1:10 and centrifuged at 8,000× *g* for 5 minutes, washed in 0.9% saline solution, and resuspended in prewarmed buffered tryptone–yeast extract broth 1.25× at pH 7.0 containing 0.5% sucrose (cell suspension 5×10⁵ CFU/mL). Biofilm-formation assays were performed using polystyrene U-bottom cell-culture plates (TPP, Trasadingen, Switzerland) following two different methods: 1) salivary preparation with each treatment was added to each well with the cell culture (salivary fluid phase), or 2) wells were first coated with salivary preparations before being inoculated with cell suspension (salivary surface-bound phase). For experiments with fluid-phase salivary preparation, 120 µL cell suspension was inoculated into the wells concomitantly with 10 µL each treatment + 30 µL saliva, maintaining the proportion of 25% saliva, as proposed by Castillo.³⁸ For experiments with surface-bound salivary preparations, each well was conditioned with each treatment diluted in saliva (1:3) and incubated at 37°C for 1 hour prior to inoculation of cell suspensions into the wells. All plates were incubated at 37°C in 5% CO₂ for 24 hours. After that, plates were washed by immersion in sterile distilled water to remove unadhered cells. After brief drying, 150 µL aqueous 1% crystal violet was added to each well, and the plates were incubated at room temperature for 30 minutes. Next, the crystalline violet solution was removed and the plates washed again. The plates were inverted on paper towels and remained for 2 hours at room temperature

to dry. The crystalline violet dye (stained biofilm) was then solubilized by incubation with 200 μL ethanol per well for 30 minutes. Then, 100 μL dye in ethanol was transferred to wells of a new microplate, and absorbance was measured at 575 nm with spectrophotometry (Eon Microplate; BioTek Instruments, Winooski, VT, USA) to quantify the biomass of the biofilm.³⁹

Cytotoxicity evaluation

Human epithelial cells from the HaCaT cell line (spontaneous immortalized nontumorigenic human keratinocyte cell line, code 341; BCRJ, Rio de Janeiro, Brazil) were cultured in DMEM (Thermo Fisher Scientific, Waltham, MA, USA) plus 10% fetal calf serum and 100 $\mu\text{g}/\text{mL}$ penicillin G–streptomycin. Cells were cultured until reaching a sub-confluent density at 37°C in a wet 5% CO_2 atmosphere. Epithelial cells were harvested following 0.25% trypsin–EDTA treatment for 5 minutes (TrypLE Express; Thermo Fisher Scientific) at 37°C. Proteases were then inactivated by adding 0.3 mg/mL trypsin inhibitor, and cells were harvested by centrifugation (500 \times g for 5 minutes), suspended in fresh medium, seeded in a 96-well microplate (200 $\mu\text{L}/\text{well}$, 10⁶ cells/mL), and incubated overnight at 37°C in a 5% CO_2 atmosphere to allow for cell adhesion before stimulation. All treatments (1 mg/mL) were diluted 1:500 in DMEM prior to their use in cell cultures. Dilutions and times of exposure were based on those reported by Guillot et al.⁴² Cells were then treated with F, p1025, F + p1025, F + Chx, and Chx for 5, 30, and 60 minutes at 37°C in a 5% CO_2 atmosphere. After exposure, the culture medium was replaced in the wells and cells again incubated for 24 hours. Then, a colorimetric MTT cell-viability assay (Hoffman-La Roche, Basel, Switzerland) was used to determine the effect of the treatments on cell viability. After 24 hours, the extracts were aspirated and replaced by 90 μL DMEM plus 10 μL MTT solution (5 mg/mL sterile PBS; Sigma-Aldrich). After that, the culture medium with MTT solution was removed and replaced with 100 μL acidified isopropanol solution (0.04 N HCl). Two 50 μL aliquots from each well were transferred to 96-well plates (Costar, Greenwich, CT, USA). Cell viability was evaluated using spectrophotometry as being proportional to the absorbance measured at 570 nm using an enzyme-linked immunosorbent-assay microplate reader (3550-UV; Bio-Rad Laboratories, Hercules, CA, USA). Means were calculated for the groups and transformed into percentages, which represented the inhibitory effect of the extracts on the mitochondrial activity of the cells. The positive control (DMEM) was defined as having 100% cell metabolism.⁴⁰

Statistical analyses

Characterizations of the formulations are presented using descriptive analysis. Microbiological and cytotoxicity assays were carried out in four replicates over 3 days ($n=12$). Results for biofilm biomass quantification ($\text{OD} - \text{Abs}_{550}$) were analyzed according to the different phases of biofilm, surface-bound salivary phase, and salivary fluid phase, with Kruskal–Wallis and Mann–Whitney tests comparing the different groups of treatments. Data from cytotoxicity assays were analyzed by analysis of variance/Tukey's tests. All tests were analyzed using SPSS version 17.1, with $P<0.05$ considered statistically significant.

Results

The ternary-phase diagram illustrated in Figure 1 shows that phase separation occurred below 40% of PPG-5-Ceteth-20 in virtually all aqueous- and oily-phase combinations. Furthermore, translucent viscous and transparent viscous systems were formed from 40% PPG-5-Ceteth-20, and the viscosity of the formulations increased starting from 40% surfactant with water addition. Based on these findings, three points named F1C, F2C, and F3C were selected from this diagram region with 40% PPG-5-Ceteth-20, because they were located in a region of viscosity transition. Alternately, with the addition of saliva, F3C showed in situ gelling to the viscous formulation F1C, which may promote higher retention and a longer

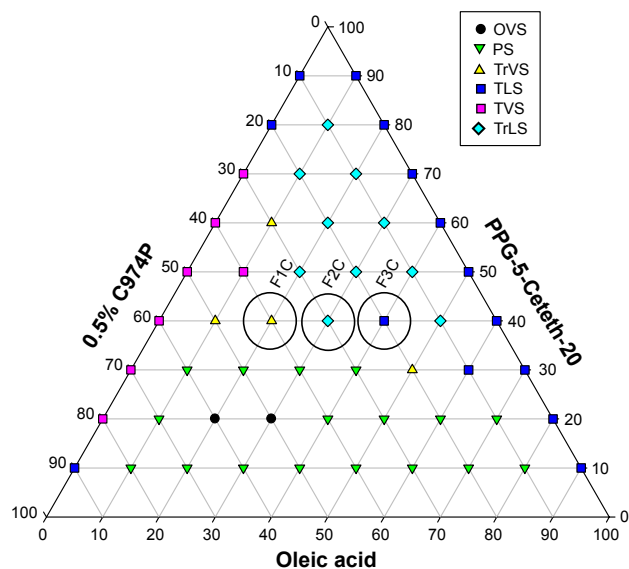


Figure 1 Ternary-phase diagram.

Notes: Polyoxypropylene-(5)-polyoxyethylene-(20)-cetyl alcohol (PPG-5-Ceteth-20), oleic acid, and 0.5% C974P dispersion (0.5% C974P). F1C, F2C, and F3C were the formulations selected for structural characterization.

Abbreviations: TLS, transparent liquid system; TrLS, translucent liquid systems; TVS, transparent viscous system; TrVS, translucent viscous system; OVS, opaque viscous system; PS, phase separation.

Table 1 Composition of formulations selected for characterization

	% OA	% PC	% W	% C974
F1C	20	40	30	10
F2C	30	40	20	10
F3C	40	40	10	10

Abbreviations: OA, oleic acid; PC, PPG-5-Ceteth-20; W, water; C974, polymer dispersion of Carbopol C974P.

release of p1025. Table 1 indicates the composition of the three selected systems.

Micrography obtained using PLM shown in Figure 2 demonstrates that F3C is a microemulsion, because it is an isotropic transparent liquid system when visualized in a dark field, while the F2C and F1C formulations are lamellar and hexagonal LC mesophases. They are anisotropic samples identified by malt crosses and striations, respectively. In order to confirm the results obtained by PLM, SAXS measurements were performed, and are shown in Figure 3. F3C presented a broad and wide peak characteristic of a microemulsion, confirming the PLM results. F1C and F2C indicated that these systems are lamellar LC mesophases, since lamellar mesophases followed the relation 2:1 and hexagonal mesophases 1:1.73:2:2.64.⁴¹ PLM showed that only F1C is a hexagonal mesophase; therefore, F1C might be in a transition phase from the lamellar to hexagonal mesophase. These data show that F3C is a precursor of the LCS and that when water is incorporated, it becomes an LCS. Therefore, the findings support our goal to develop a flow formulation to facilitate administration with a syringe, which upon contact with saliva would become a viscous LC mesophase.

Table 2 shows the distance between lamellae:

$$d = \frac{2p}{q_{\max}} \quad (4)$$

where d is correlation distance and q_{\max} is the value of the scattering vector q at maximum intensity used to calculate the spacing between the lamellae. It was observed that d increased with water amount (7.75–7.85 nm), suggesting

polarization of the polar head of the surfactant by the addition of water. This led to an increase in curvature and volume of the polar region, resulting in the generation of hexagonal structures because of greater packaging.

The flow-rheology data for F1C, F2C, and F3C are shown in Figure 4 and Table 3. The data showed that both F1C and F2C exhibited non-Newtonian pseudoplastic behavior ($n < 1$), whereas F3C exhibited Newtonian behavior ($n = 1$). Furthermore, the consistency index increased with the addition of water, indicating that F1C is a more viscous formulation. The F1C downward curve did not overlap its upward curve, instead forming an area of hysteresis, and was thus classified as time-dependent thixotropic.

Figure 5 and Table 4 show the oscillatory rheology data. F1C had a G' value higher than the G'' value, a characteristic of elastic formulations. F2C and F3C had higher G'' values than G' values, indicating the predominantly viscous behavior characteristic of poorly organized systems. Moreover, the S value of F1C was much higher than that of the other formulations, demonstrating that the bonds among the molecules of F1C are much more resistant.

Table 5 shows the results of the bioadhesion test, indicating that F1C had higher bioadhesion strength than F2C and F3C, suggesting that bioadhesion was strongly influenced by the type of LC mesophase. Results for the quantification of biofilm biomass in the two different phases of biofilm – surface-bound salivary phase and salivary fluid-phase – are shown in Figures 6 and 7, respectively. All treatments affected biofilm formation when applied in the surface-bound salivary phase. The best antibiofilm effects were observed for F + p1025 and F + Chx, without a statistical difference between them. When applied in the salivary fluid phase, p1025 had no effect on biofilm formation. There were no statistical differences among the F groups (F, F + p1025, and F + Chx). F + Chx had the greatest effect on biofilm formation.

Data from cytotoxicity are presented in Figure 8. Chx and p1025 solutions were not cytotoxic at any time evaluated. F increased its toxicity when exposure time increased. There was no statistical difference among exposure times for

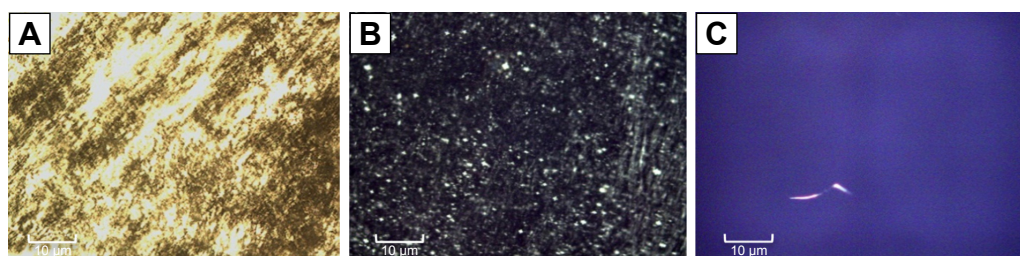


Figure 2 Polarized light microscopy of formulations F1C (A), F2C (B), and F3C (C). Magnification 20×.

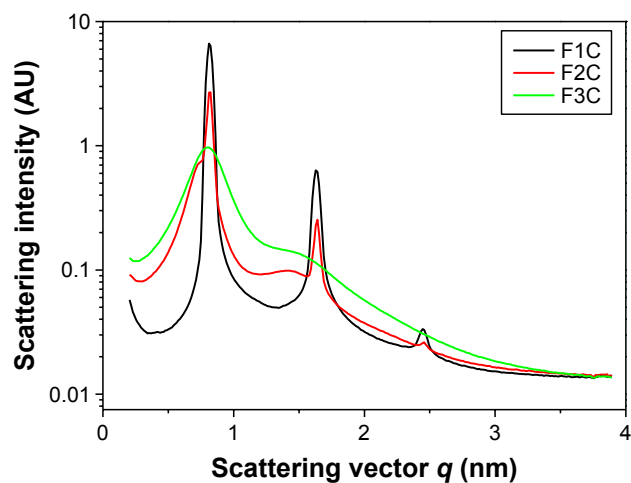


Figure 3 Small-angle X-ray scattering results obtained for formulations F1C, F2C, and F3C.

F + p1025. After 30 and 60 minutes, the toxicity of F + Chx increased significantly when compared with toxicity at 5 minutes. Overall, cell viability was 70% or higher for F, F + p1025, and F + Chx, independently of the time of exposure, showing low cytotoxicity for all the treatments.

Discussion

We aimed to develop a bioadhesive LCS with in situ gelling properties to prevent the formation of *S. mutans* biofilm. For this reason, a phase diagram was constructed to determine the percentages of surfactant, oily phase, and aqueous phase required to obtain an LC-precursor system that (with the addition of water) could transform to an LCS for topical administration to the teeth.

After analysis of the phase diagram, it was possible to verify the formation of a fluid system and viscous system beyond phase separation. Specifically, in the region of 40% surfactant, it was possible to obtain a transition phase with the addition of the aqueous phase. In this region, formulations have low concentrations of surfactant, in order to decrease their potential toxicity.³³ Then, three formulations (F1C, F2C, and F3C) in this region were structurally analyzed by PLM, SAXS, rheology, and bioadhesion studies. PLM and SAXS showed that combining PPG-5-Ceteth-20, OA, 0.5% C974 dispersion, and water formed an LCS after the addition of water.

Table 2 Values of q_{\max} (Å) and distance (d) between lamellae

	$q_{\max 1}$	$q_{\max 2}$	$q_{\max 3}$	d (nm)
F1C	0.81	1.62	2.43	7.85
F2C	0.83	1.62	2.45	7.75
F3C	NA	NA	NA	NA

Abbreviations: q_{\max} , maximum intensity of scattering vector q ; NA, not applicable.

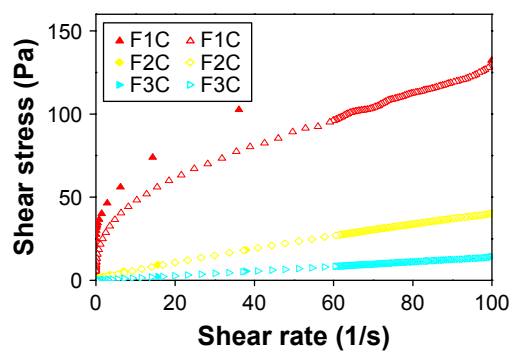


Figure 4 Flow properties of formulations F1C, F2C, and F3C.

Notes: The flow properties were determined using a controlled shear rate procedure ranging from 0.01 to 100 s^{-1} (or ascendent curve – filled symbols) and back (or descendant curve – empty symbols).

The flow-rheology study showed that the LCSs (F1C and F2C) are pseudoplastic fluids and the microemulsion (F3C) is a Newtonian fluid. The microemulsions had Newtonian behavior, since they did not present any type of organized structure that could be disassembled by shear stress.⁴³ However, pseudoplasticity can be due to the LC structure, which causes greater resistance to flow than the microemulsions, which are colloidal systems.⁴⁴ Such a property is desirable for formulations developed for oral administration, eg, during application at high shear rates, deinterlacing of the polymer chains, and subsequent thinning of the flow will occur, thereby facilitating administration of the formulation. However, upon withdrawal of this tension, the formulation will recover its initial viscosity, remaining longer in the oral environment.

F2C and F3C presented a very low degree of thixotropy. However, the formulation F1C presented a high degree of thixotropy. Thixotropic properties were directly related to the interaction between the components of the formulation. Because of the existence of interaction forces between the more structured regions, the structure can be destroyed by increasing the shear rate and easily recovered when that speed decreases. Therefore, the formulations with the highest degree of thixotropy also presented a higher degree of initial structuring. This increase in hysteresis is closely related to the increase in the microstructure of the LC networks, proving that hysteresis is strongly influenced by the presence of LC.⁴⁵

Table 3 Flow behavior (n) and consistency index (κ) of the formulations

	n	κ
F1C	0.3	34.47
F2C	0.76	1.18
F3C	1	0.15

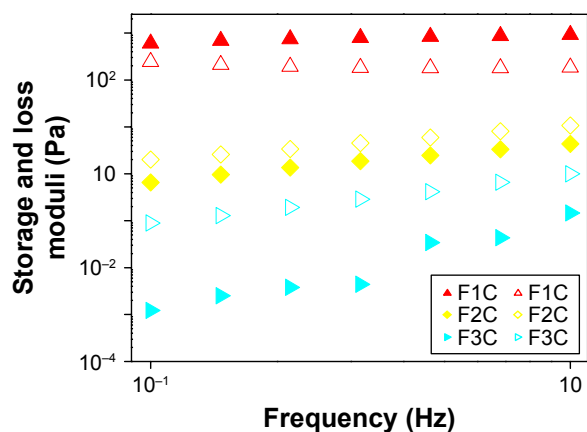


Figure 5 Variations in storage moduli (G' ; filled symbols) and loss moduli (G'' ; empty symbols) as a function of frequency for F1C, F2C, and F3C.

Oscillatory rheological analysis evaluates the viscoelastic properties of formulations and provides information about their structural nature, which directly affects their performance.⁴⁶ F2C and F3C had G'' value that were higher than G' values, indicating a predominantly viscous behavior, a characteristic of poorly organized systems. In contrast, F1C showed a highly elastic character. The lamellar phase generally appears as viscous liquid, and the hexagonal phase has a gel-like viscosity. Therefore, the rheological data corroborated the SAXS analysis, showing that when the aqueous phase increased, the system structure became more ordered, as indicated by the increase in lamellae spacing and elasticity.^{47,48}

The main advantage of bioadhesive systems for drug delivery is maintenance of the drug at the application site for longer periods, which allows for enhanced contact of the formulation with the biological barrier, allowing for a reduction in the frequency of product application and increasing patient compliance.⁴⁹ The bioadhesion results showed that the increase in the aqueous phase in the systems significantly increased the bioadhesion of the formulations, due to the formation of LC. The highest values of bioadhesion for the LCS can be explained by their rheological properties. The increase in viscosity and elastic characteristics contributes to the increase in the residence time of the formulation.⁴⁴

Furthermore, bioadhesion can be also attributed to presence of the negatively charged polymer C974. Although the literature reports that chitosan hydrogels are very bioadhesive due to the forces of molecular attraction by electrostatic

Table 4 Strength (S) and the viscoelastic exponent (n) of the formulations

	S	n
F1C	933	0.16
F2C	4.39	0.77
F3C	0.14	2.57

Table 5 Work of bioadhesive force (mN·s) of the formulations. Values represent mean \pm SD at 37°C

Formulations	Bioadhesive strength
F1C	26.29 \pm 3.15
F2C	12.84 \pm 2.14
F3C	11.23 \pm 0.7

interactions between positive groups of chitosan and negative groups of the biological surface, we were able to demonstrate that the F1C obtained values within the range of bioadhesion for chitosan-based LCS values.³³ In this case, bioadhesion was attributable to physicochemical processes, such as hydrophobic interactions, hydrogen, and van der Waals interactions, which are controlled by pH and ionic composition.⁵⁰ In addition, their chains are flexible enough to diffuse into the saliva and penetrate to form a network. Most of the polyacrylic acid derivatives are not soluble in water, but form viscous gels when hydrated, increasing their ability to adhere to the tooth surface.⁴⁴

There is no standard formula available for bioadhesive drug-delivery systems for dental applications. However, the LCS formed by the C974 polymer as an aqueous phase was shown to be suitable, because upon hydration there was an increase in bioadhesion strength, pseudoplasticity, and elasticity, resulting in a promising platform for oral p1025 delivery.

In this study, p1025, a peptide that corresponds to residues 1025–1044 in the C-terminal region of SA I/II, was chosen to be incorporated into LCS. Marsh et al (2015) suggested that a delicate balance is needed to control microbiota at levels

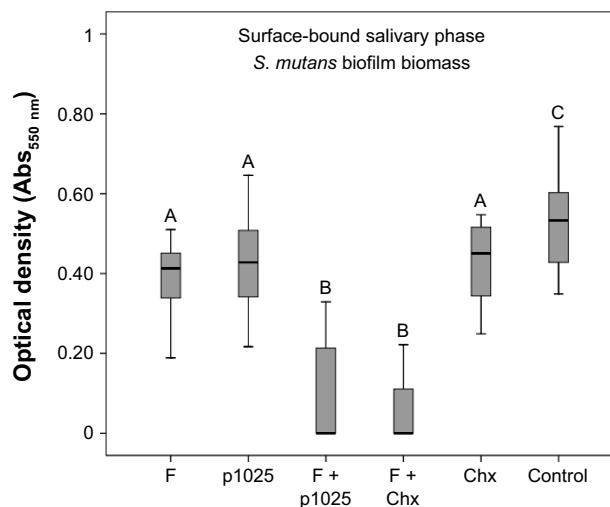


Figure 6 Quantification of *Streptococcus mutans* biofilm biomass after 24 hours treatment in the surface-bound salivary phase.

Notes: Bars indicate minimum and maximum values. Boxes indicate lower and upper quartiles, respectively. Lines in the middle of boxes are medians ($n=12$). Different uppercase letters indicate statistical differences among the groups, according to Kruskal–Wallis/Mann–Whitney tests ($P<0.05$).

Abbreviations: F, liquid-crystalline formulation; p1025, peptide p1025; Chx, chlorhexidine.

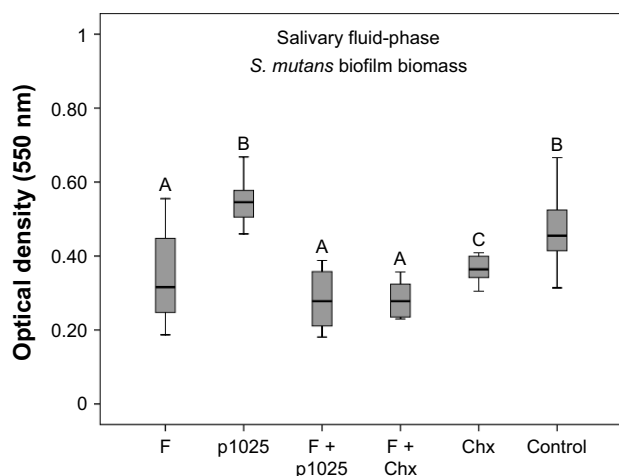


Figure 7 Quantification of *Streptococcus mutans* biofilm biomass 24 hours after treatment in the salivary fluid phase.

Notes: Bars indicate minimum and maximum values. Boxes indicate lower and upper quartiles, respectively. Lines in the middle of boxes are medians (n=12). Different uppercase letters indicate statistical differences among the groups, according to Kruskal–Wallis/Mann–Whitney tests ($P < 0.05$).

Abbreviations: F, liquid-crystalline formulation; p1025, peptide 1025; Chx, chlorhexidine.

compatible with health, using substances able to inhibit bacterial traits implicated in disease and retard growth without eliminating beneficial species.⁵¹ Thus, in this present study, p1025, a peptide that corresponds to residues 1025–1044 in the C-terminal region of SA I/II, was chosen to be incorporated into LCS, because p1025 is able to inhibit the binding between *S. mutans* and salivary agglutinin, reducing adhesion and consequent biofilm formation.¹⁸

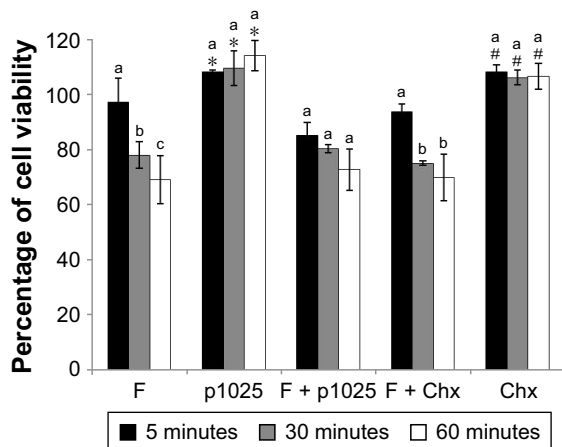


Figure 8 Epithelial cell viability after 5, 30, and 60 minutes of treatment and growth for 24 hours.

Notes: *Significant difference between p1025 and the other groups (F, F + p1025, F + Chx), except for Chx, considering each time of exposure separately, according to ANOVA/Tukey's tests; #significant difference between Chx and the other groups (F, F + p1025, F + Chx), except for p1025, considering each time of exposure separately, according to ANOVA/Tukey's tests. Columns indicate means and bars indicate standard deviations (n=12). Different letters show significant differences among times of exposure (5, 30, or 60 minutes), considering each group separately, according to ANOVA/Tukey's tests.

Abbreviations: F, liquid-crystalline formulation; p1025, peptide p1025; Chx, chlorhexidine; ANOVA, analysis of variance.

In the present study, when applied in the salivary surface-bound phase, p1025, whether or not it was incorporated into the LCS, showed an inhibitory effect on biofilm formation. It is known that synthetic peptide p1025 is able to bind to salivary agglutinins and interfere with *S. mutans* adhesion mediated by SA I/II, as confirmed by surface plasmon resonance.¹⁸ However, this effect was not observed when p1025 was applied in the salivary fluid-phase. It is possible that p1025 attached to salivary agglutinins is not degraded as easily by salivary proteases as it is in the fluid-phase.

Data from literature reports reveal that the release of agents from the LCS is around 4% at 24 h.⁵² Although data from the release of antimicrobial agents were not available in the present study, the peptide and Chx release from LCS was probably higher than 4%, since the formulation was diluted previously to reduce viscosity and incorporate antimicrobial agents for biofilm assays.

There was an increase in the anti-biofilm activity of F+p1025 compared to p1025 and F+Chx compared to Chx within 24 h, showing a cumulative effect of these agents when incorporated into F. This result may suggest that p1025 and Chx were released slowly within 24 h, since the mean bacterial reduction was around 20% for p1025/Chx and 80% for F+p1025/F+Chx. Lower bacterial reduction (around 40%) was observed for both F containing p1025 or Chx when applied in the salivary fluid-phase, and this was probably related to dilution in the saliva.

An additional antimicrobial effect of F (around 27%) was observed from the biofilm assays, adding to the effect of F (around 27%) was observed from the biofilm assays, adding to the effect of the incorporated agents. The high concentration of oil in the LCS limits water access, which is one of the main methods of antimicrobial action.⁵³

There are few studies evaluating the inhibitory activity of p1025 on pathogenic microorganisms related to dental caries etiology. Kelly et al demonstrated that topical application of p1025 might selectively prevent recolonization of the tooth surface by *S. mutans*.¹⁸ The relatively long-term resistance to colonization cannot be explained by persistence of the peptide in the oral cavity. The authors suggested that the peptide competitively inhibited initial adhesion of the bacterium to the dental structure, but other bacteria competing for the same ecological niche were able to prevent subsequent colonization. Li et al evaluated the influence of p1025 in solution and two different dentifrices containing p1025 on the adherence of *S. mutans*, and observed an inhibitory effect in both hydroxyapatite (in vitro) and dental biofilm (in vivo).¹⁹ The most significant inhibitory activity in vitro was shown at 50 $\mu\text{mol/L}$. The clinical efficacy of the dentifrices was confirmed by the

significant reduction in plaque scores and *S. mutans* counts from subjects after 1 month's treatment with dentifrices containing p1025 in comparison to a control dentifrice.

No study has evaluated the toxicity of p1025 or this formulation of LCS against eukaryotic cells. In the present study, p1025 was not toxic for epithelial cells; however, when it was incorporated into the LCS, there was a significant reduction in cell viability, although viability was maintained at around 70% until 1 hour of exposure. Considering the high capacity of pathogenic bacteria for developing resistance to current antimicrobial agents, the topical administration on teeth of the p1025-loaded LCS, a clinically appropriate and safe formulation, provides a realistic adjunctive approach to prevention of the formation of *S. mutans* dental biofilm.

Conclusion

An LCS was successfully developed combining polyoxypropylene-(5)-polyoxyethylene-(20)-cetyl alcohol, OA, and C974P dispersion. Characterization tests revealed that the addition of water caused a phase transition consisting of the formation of a hexagonal LC mesophase with pseudo-plasticity, high viscosity, and superior bioadhesion to the teeth. The p1025-loaded LCS showed limited cytotoxicity and presented an effect against the formation of *S. mutans* biofilm. Taken together, the results suggest that this p1025-loaded LCS offers a promising alternative for the prevention of *S. mutans* biofilm. Future in vivo studies are needed to evaluate the efficiency of this approach.

Acknowledgments

This study was funded by Fundação de Amparo à Pesquisa do Estado de São Paulo (FAPESP) grants 2012/19235-5, 2013/12285-0, and 2013/01565-1, CNPq, and PADC (Programa de Apoio ao Desenvolvimento Científico-FCF-UNESP).

Disclosure

The authors report no conflicts of interest in this work.

References

- Hahnel S, Mühlbauer G, Hoffmann J, et al. *Streptococcus mutans* and *Streptococcus sobrinus* biofilm formation and metabolic activity on dental materials. *Acta Odontol Scand*. 2012;70(2):114–121.
- Alam S, Brailsford SR, Adams S, et al. Genotypic heterogeneity of *Streptococcus oralis* and distinct aciduric subpopulations in human dental plaque. *Appl Environ Microbiol*. 2000;66(8):3330–3336.
- Hamada S, Slade HD. Biology immunology, and cariogenicity of *Streptococcus mutans*. *Microbiol Rev*. 1980;44(2):331–384.
- Lagerweij MD, van Loveren C. Declining caries trends: are we satisfied? *Curr Oral Health Rep*. 2015;2(4):212–217.
- Marsh PD. Role of the oral microflora in health. *Microb Ecol Health Dis*. 2000;12(3):130–137.
- Marsh PD. Dental plaque as a biofilm and a microbial community: implications for health and disease. *BMC Oral Health*. 2006;6:S14.
- Loesche WJ. Microbiology of dental decay and periodontal disease. In: Baron S, editor. *Medical Microbiology*. 4th ed. Galveston (TX): University of Texas; 1996.
- Filoché S, Wong L, Sissons CH. Oral biofilm: emerging concepts in microbial ecology. *J Dent Res*. 2010;89(1):8–18.
- Russell MW, Bergmeier LA, Zanders ED, Lehner T. Protein antigens of *Streptococcus mutans*: purification and properties of a double antigen and its protease-resistant component. *Infect Immun*. 1980;28(2):486–493.
- Smith R, Lehner T, Beverley PC. Characterization of monoclonal antibodies to *Streptococcus mutans* antigenic determinants III, I, II, and III and their serotype specificities. *Infect Immun*. 1984;46(1):168–175.
- Lee SF, Progulské-Fox A, Bleiweis AS. Molecular cloning and expression of a *Streptococcus mutans* major surface protein antigen, P1 (I/II), in *Escherichia coli*. *Infect Immun*. 1988;56(8):2114–2119.
- Smith DJ. Caries vaccines for the twenty-first century. *J Dent Educ*. 2003;67(10):1130–1139.
- Robinette RA, Heim KP, Oli MW, Crowley PJ, McArthur WP, Brady LJ. Alterations in immunodominance of *Streptococcus mutans* Ag I/II: lessons learned from immunomodulatory antibodies. *Vaccine*. 2014;32(3):375–382.
- Younson J, Kelly C. The rational design of an anti-caries peptide against *Streptococcus mutans*. *Mol Divers*. 2004;8(2):121–126.
- Sanui T, Gregory RL. Analysis of *Streptococcus mutans* biofilm proteins recognized by salivary immunoglobulin A. *Oral Microbiol Immunol*. 2009;24(5):361–368.
- Pecharki D, Petersen FC, Assev S, Scheie AA. Involvement of antigen I/II surface proteins in *Streptococcus mutans* and *Streptococcus intermedius* biofilm formation. *Oral Microbiol Immunol*. 2005;20(6):366–371.
- Carlén A, Olsson J. Monoclonal antibodies against a high-molecular-weight agglutinin block adherence to experimental pellicles on hydroxyapatite and aggregation of *Streptococcus mutans*. *J Dent Res*. 1995;74(4):1040–1047.
- Kelly CG, Younson JS, Hikmat BY, et al. A synthetic peptide adhesion epitope as a novel antimicrobial agent. *Nat Biotechnol*. 1999;17(1):42–47.
- Li MY, Wang J, Lai GY. Effect of a dentifrice containing the peptide of streptococcal antigen I/II on the adherence of mutans streptococcus. *Arch Oral Biol*. 2009;54(11):1068–1073.
- Souza C, Watanabe E, Borgheti-Cardoso LN, Fantini MC, Lara MG. Mucoadhesive system formed by liquid crystals for buccal administration of poly(hexamethylene biguanide) hydrochloride. *J Pharm Sci*. 103(12):3914–3923.
- Bernegossi J, Calixto GM, Sanches PR, et al. Peptide KSL-W-loaded mucoadhesive liquid crystalline vehicle as an alternative treatment for multispecies oral biofilm. *Molecules*. 2015;21(1):E37.
- Bernegossi J, Calixto G, Fonseca-Santos B, et al. Highlights in peptide nanoparticle carriers intended to oral diseases. *Curr Top Med Chem*. 2015;15(4):345–355.
- Gajdziok J, Bajerová M, Chalupová Z, Rabisková M. Oxycellulose as mucoadhesive polymer in buccal tablets. *Drug Dev Ind Pharm*. 2010;36(9):1115–1130.
- Lofstson T, Leeves N, Bjornsdottir B, Duffy L, Masson M. Effect of cyclodextrins and polymers on triclosan availability and substantivity in toothpastes in vivo. *J Pharm Sci*. 1999;88(12):1254–1258.
- Guo C, Wang J, Cao F, Lee RJ, Zhai G. Lyotropic liquid crystal systems in drug delivery. *Drug Discov Today*. 2010;15(23–24):1032–1040.
- Calixto G, Bernegossi J, Fonseca-Santos B, Chorilli M. Nanotechnology-based drug delivery systems for treatment of oral cancer: a review. *Int J Nanomedicine*. 2015;9:3719.
- de Souza AL, Kiill CP, dos Santos FK, et al. Nanotechnology-based drug delivery systems for dermatomycosis treatment. *Curr Nanosci*. 2012;8(4):512–519.
- Calixto GM, Garcia MH, Cilli EM, Chiavacci LA, Chorilli M. Design and characterization of a novel p1025 peptide-loaded liquid crystalline system for the treatment of dental caries. *Molecules*. 2016;21(2):158.

29. Bruschi ML, de Freitas O, Lara EH, Panzeri H, Gremião MP, Jones DS. Precursor system of liquid crystalline phase containing propolis microparticles for the treatment of periodontal disease: development and characterization. *Drug Dev Ind Pharm*. 2008;34(3):267–278.
30. Calixto G, Yoshii AC, Rocha e Silva H, Cury BS, Chorilli M. Polyacrylic acid polymers hydrogels intended to topical drug delivery: preparation and characterization. *Pharm Dev Technol*. 2015;20(4):490–496.
31. Carvalho FC, Calixto G, Hatakeyama IN, Luz GM, Gremião MP, Chorilli M. Rheological, mechanical, and bioadhesive behavior of hydrogels to optimize skin delivery systems. *Drug Dev Ind Pharm*. 2013;39(11):1750–1757.
32. Jones DS, Bruschi ML, de Freitas O, Gremião MP, Lara EH, Andrews GP. Rheological, mechanical and mucoadhesive properties of thermoresponsive, bioadhesive binary mixtures composed of poloxamer 407 and carbopol 974P designed as platforms for implantable drug delivery systems for use in the oral cavity. *Int J Pharm*. 2009;372(1):49–58.
33. Salmazi R, Calixto G, Bernegossi J, Ramos MA, Bauab TM, Chorilli M. Curcumin-loaded liquid crystalline precursor mucoadhesive system for the treatment of vaginal candidiasis. *Int J Nanomedicine*. 2015;10:4815–4824.
34. Soares DG, Ribeiro AP, Sacono NT, Coldebella CR, Hebling J, Costa CA. Transenamel and transdentinal cytotoxicity of carbamide peroxide bleaching gels on odontoblast-like MDPC-23 cells. *Int Endod J*. 2011;44(2):116–125.
35. Marques MR, Loebenberg R, Almukainzi M. Simulated biological fluids with possible application in dissolution testing. *Dissolut Technol*. 2011;18(3):15–28.
36. Gawande PV, Leung KP, Madhyastha S. Antibiofilm and antimicrobial efficacy of Dispersin B KSL-W peptide-based wound gel against chronic wound infection associated bacteria. *Curr Microbiol*. 2014;68(5):635–641.
37. Ahn SJ, Wen ZT, Brady LJ, Burne RA. Characteristics of biofilm formation by *Streptococcus mutans* in the presence of saliva. *Infect Immun*. 2008;76(9):4259–4268.
38. Castillo MC. *Função de DNA Extracelular e de Acido Lipoteicoico nas Propriedades Estruturais e Funcionais da Matriz Extracelular de Biofilmes Cariogênicos* [master's thesis]. São Paulo: São Paulo State University; 2016.
39. Mattos-Graner RO, Napimoga MH, Fukushima K, Duncan MJ, Smith DJ. Comparative analysis of Gtf isozyme production and diversity in isolates of *Streptococcus mutans* with different biofilm growth phenotypes. *J Clin Microbiol*. 2004;42(10):4586–4592.
40. Bedran TB. Efeito antimicrobiano e modulador da resposta imune dos peptídeos hBD-3 e LL-37 e dos polifenóis o chá verde e do cranberry. 2014. Available from: <https://repositorio.unesp.br/handle/11449/124090>. Accessed October 19, 2017.
41. Oyafuso MH, Carvalho FC, Takeshita TM, et al. Development and in vitro evaluation of lyotropic liquid crystals for the controlled release of dexamethasone. *Polymers*. 2017;9(8):330.
42. Guillot S, Méducin F, Poljak K, et al. Nanostructured monolinolein mini-emulsions as delivery systems: role of the internal mesophase on cytotoxicity and cell internalization. *Int J Pharm*. 2017;523(1):142–150.
43. Pénzes T, Ildikó CsókaIstván Erős. Rheological analysis of the structural properties effecting the percutaneous absorption and stability in pharmaceutical organogels. *Rheol Acta*. 2004;43(5):457–463.
44. Carvalho FC, Silva HR, da Luz GM, et al. Rheological, mechanical and adhesive properties of surfactant-containing systems designed as a potential platform for topical drug delivery. *J Biomed Nanotechnol*. 2012;8(2):280–289.
45. Chorilli M, Prestes PS, Rigon RB, et al. Structural characterization and in vivo evaluation of retinyl palmitate in non-ionic lamellar liquid crystalline system. *Colloids Surf B Biointerfaces*. 2011;85(2):182–188.
46. Chorilli M, Rigon RB, Calixto G, et al. Rheological characterization and safety evaluation of non-ionic lamellar liquid crystalline systems containing retinyl palmitate. *J Biomed Nanotechnol*. 2016;12(2):394–403.
47. Gabboun NH, Najib NM, Ibrahim HG, Assaf S. Release of salicylic acid and diclofenac acid salts from isotropic and anisotropic nonionic surfactant systems across rat skin. *Int J Pharm*. 2001;212(1):73–80.
48. Cintra GA, Pinto LA, Calixto GM, et al. Bioadhesive surfactant systems for methotrexate skin delivery. *Molecules*. 2016;21(2):E231.
49. Smart JD, Riley RG, Tsibouklis J, et al. The retention of ¹⁴C-labelled poly(acrylic acids) on gastric and oesophageal mucosa: an in vitro study. *Eur J Pharm Sci*. 2003;20(1):83–90.
50. Woodley J. Bioadhesion: new possibilities for drug administration? *Clin Pharmacokinet*. 2001;40(2):77–84.
51. Marsh PD, Head DA, Devine DA. Ecological approaches to oral biofilms: control without killing. *Caries Res*. 2015;49 Suppl 1:46–54.
52. Hu FQ, Hong Y, Yuan H. Preparation and characterization of solid lipid nanoparticles containing peptide. *Int J Pharm*. 2004;273(1–2):29–35.
53. Oliveira TA, Paixão FG, Prestes OS, et al. Avaliação da atividade antimicrobiana de sistemas nanoestruturados. *Lat Am J Pharm*. 2007;26(6):878–882.

International Journal of Nanomedicine

Publish your work in this journal

The International Journal of Nanomedicine is an international, peer-reviewed journal focusing on the application of nanotechnology in diagnostics, therapeutics, and drug delivery systems throughout the biomedical field. This journal is indexed on PubMed Central, MedLine, CAS, SciSearch®, Current Contents®/Clinical Medicine,

Submit your manuscript here: <http://www.dovepress.com/international-journal-of-nanomedicine-journal>

Dovepress

Journal Citation Reports/Science Edition, EMBase, Scopus and the Elsevier Bibliographic databases. The manuscript management system is completely online and includes a very quick and fair peer-review system, which is all easy to use. Visit <http://www.dovepress.com/testimonials.php> to read real quotes from published authors.